Proceedings of the 17th World Congress
The International Federation of Automatic Control
Seoul, Korea, July 6-11, 2008

Optimal Guidance of Unmanned Aerial Vehicles for Emitter Location ⋆

Kun Huang, N. Eva Wu, Mark L. Fowler ∗

∗ *Binghamton University, SUNY, Binghamton, NY 13790, USA (e-mail: khuang2,evawu,mfowler@binghamton.edu)*

Abstract: This paper provides a solution to guidance of multiple unmanned aerial vehicles that carry sensors for locating a detected emitter of radio frequency signals. Guidance in this paper refers to updating the state of each vehicle to the most desirable position and velocity, reachable within a given time for the location purpose. The vehicles can then be guided to the updated sensor states for further target data acquisition and processing. This process continues until the target is located within a specified accuracy. Both the guidance criterion and the vehicle state update procedure take the probability of vehicle loss into consideration. Vehicle state update is formulated and solved as an optimization problem. The enhanced location performance under the optimized guidance, and the sensor system tolerance to vehicle loss are shown for a four-sensor system through simulations.

Keywords: sensing, localization, multi-vehicle systems, fault tolerance, guidance, autonomous systems

1. INTRODUCTION

This paper establishes an entropy-based criterion as an approximate accuracy evaluation of an estimated emitter location. This criterion is shown in (Wu, et al., 2008) to be consistent with the common accuracy measure using concentration ellipses. The criterion is used to determine a set of future positions and velocities of unmanned aerial vehicles (UAV)referred to as vehicle states hereafter, reachable by individual UAVs from their current states within a time limit, based on the current estimate of the emitter. The vehicles are then guided to these states to acquire more emitter data for improved location accuracy. These future states are calculated by solving an optimization problem under the entropy-based criterion. The sensor system tolerance to loss of vehicles is discussed. Error ellipses are calculated based on the outcomes of a large number of simulations to verify the location accuracy improvement and the system tolerance to vehicle loss.

This paper considers the use of a specific location technology where time difference of arrival (TDOA) and frequency difference of arrival (FDOA) are measured by paired sensors. Each sensor is carried by a UAV. Emitter location accuracy using TDOA/FDOA measurements was analyzed by Chesnut [1982], where the relation between the emitter location accuracy as a function of FDOA/TDOA measurement accuracy, and the sensor position and velocity was provided. Torrieri [1984] gave an overview of some statistical methods for the analysis of a number of passive location systems. Day et al. [1989] introduced a general covariance error model for TDOA/FDOA measurement, where many sources of errors were encompassed. Ho et al. [2004] provided an analytic solution for TDOA/FDOA measurements under the far-field assumption, which is also made in this paper for calculating vehicle state updates. In general, technologies for TDOA/FDOA sensing and emitter location estimation based on the measurement data are well understood and readily available.

UAV guidance has been discussed by Kaminer et al. [2006], and Yakimenko [2000] as a combined guidance and control problem involving feasible trajectory generation, path following, and time-critical coordination of UAVs, for which a solution is proposed to ensure collision-free maneuvers under strict spatial and temporal constraints. This technique is highly relevant to our target location problem involving coordinated airborne sensors. Application of this technique is being considered for our next step of investigation that progresses from guidance to control of vehicles. The issue addressed in this paper concerns, however, only how to guide a group of UAVs that are subject to failures during a location mission for the best quality of acquired emitter data.

The reminder of this paper is organized as follows. Section 2 presents the background of TDOA/FDOA location technology and introduces the criterion for UAV guidance. Section 3 focuses on setting the guidance problem into an optimization problem. In particular, the guidance problem is generalized to include the consideration of probability of loss of vehicles, and to allow the network reorganization upon loss of vehicles. Following the principles described in (Wu, et al., 2008), section 4 reports simulation results performed for a system of four guided sensors under the proposed guidance criterion to demonstrate the enhanced location accuracy, and tolerance to loss of vehicles. Section 5 concludes the paper.

⋆ The authors acknowledge the support of this work by the AFOSR under Grants FA9550-06-0456 and FA9550-06-1-0249.

2. PROBLEM DESCRIPTION

Suppose that one pair of UAVs collects collaboratively both time difference of arrival (TDOA) and frequency difference of arrival (FDOA) data from an RF emitter. If there is no error in the measurements, the emitter location can be solved from (1) and (2) below. Let (x_e, y_e) be the emitter location, (x_1, y_1), (x_2, y_2), (u_1, v_1), and (u_2, v_2) be the positions and velocities of the two sensors, respectively. Let f_e denote the radio frequency (RF) of the emitter and c denote the speed of light. a noiseless TDOA measurement from the two sensors is

$$f_{TDOA} = \frac{1}{c}[\sqrt{(x_1 - x_e)^2 + (y_1 - y_e)^2} - \sqrt{(x_2 - x_e)^2 + (y_2 - y_e)^2}], \quad (1)$$

and a noiseless FDOA measurement from two sensors is

$$f_{FDOA} = \frac{f_e}{c}[\frac{(x_1 - x_e)u_1 + (y_1 - y_e)v_1}{\sqrt{(x_1 - x_e)^2 + (y_1 - y_e)^2}} - \frac{(x_2 - x_e)u_2 + (y_2 - y_e)v_2}{\sqrt{(x_2 - x_e)^2 + (y_2 - y_e)^2}}]. \quad (2)$$

To be more realistic, each signal received at a sensor can be modeled as an ideal time/frequency measurement corrupted by an additive Gaussian noise. The signals from two sensors are cross-correlated to obtain the maximum likelihood estimates of the TDOA and the FDOA for that pair (Stein, 1993). With large number of signal samples, the TDOA/FDOA estimates can be assumed to be Gaussian and their error covariance achieves the Cramer-Rao lower bound (CRLB) by invoking the asymptotic properties of maximum likelihood estimate (Kay, 1993).

The error covariance matrix of the location estimate from the i^{th} pair of sensors is given by Day et al. [1989]

$$[G_i^T C_i^{-1} G_i]^{-1}, \ \ G_i = \begin{pmatrix} \frac{\partial f_{i,TDOA}}{\partial x_e} & \frac{\partial f_{i,TDOA}}{\partial y_e} \\ \frac{\partial f_{i,FDOA}}{\partial x_e} & \frac{\partial f_{i,FDOA}}{\partial y_e} \end{pmatrix}. \quad (3)$$

In a network of k pairs of sensors without sensor sharing among the pairs, the error covariance of the estimate becomes: (Fowler and Chen, 2006)

$$\left[\sum_{i=1}^{k} G_i^T C_i^{-1} G_i\right]^{-1}. \quad (4)$$

Since G_i depends on sensor states $(x_{ji}, y_{ji}, u_{ji}, v_{ji})$ through $f_{i,TDOA}$ and $f_{i,FDOA}$, $j = 1, 2$ and $i = 1, \cdots, k$, as seen in (1) and (2), the accuracy of location estimation captured in (3) and (4) is thus affected by the sensor states.

This paper uses a scalarized measure of error covariance (4) as the criterion for sensor state adjustment to enhance the accuracy of location estimation. To that end, differential entropy (Cover, et al., 1991), or entropy, for short, is chosen as the scalarized measure of covariance (4) of the Gaussian distribution of the random vector representing the estimation error in emitter location

$$\frac{1}{2}ln(2\pi e) + ln\left|(\sum_{i=1}^{k} G_i^T C_i^{-1} G_i)^{-1}\right|, \quad (5)$$

where $|.|$ denotes determinant.

Low entropy implies that the random vector, which is the error of location estimate, is confined to a small effective volume. Thus, reducing entropy improves the accuracy of location estimation. The analysis suggests that, conditioned on the most recent location estimate $(\hat{x}_e, \hat{y}_e)$, the states of the sensor-carrying UAVs can be updated to the minimizing solution of

$$\begin{cases} \min_{(x_{ji}, y_{ji}, u_{ji}, v_{ji})} \ln\left|(\sum_{i=1}^{k} G_i^T C_i^{-1} G_i)^{-1}\right| \\ \text{Subject to}: (x_{ji}, y_{ji}, u_{ji}, v_{ji}) \in \mathcal{R}_i, \ j = 1, 2, \ i = 1, \cdots, k \end{cases} \quad (6)$$

where $\mathcal{R}_{ji}$ is the reachable set of the jth UAV in the ith sensor pair, defined as the 4-dimensional convex set that can be reached by the UAV from the current state within a prescribed time interval under some predefined magnitude limits of speed and acceleration. Issues related to the calculation of reachable sets will be reported in the near future in a separate paper.

3. ROBUST UAV GUIDANCE

This section discusses updating sensor states using entropy-based criterion (6) within a prescribed interval over which the reachable sets $\{R_{j,i}\}$ have been obtained, conditioned on the most recent location estimate. The goal is to attain the most improvement in the next cycle of TDOA/FDOA acquisition for emitter localization.

Such pursuit is then extended to situations where probability p of loss of a sensor in a given update interval is available. To improve average network performance, entropy-based criteria for all possible outcomes are weighted by their probabilities of occurrence. The section also treats sensor loss as a deterministic state information feedback problem in which a single surviving sensor is reassigned to pair with one of the sensors of an intact pair.

3.1 Guidance with optimized velocity

It is not difficult to see that (6) presents a complex problem. Two practically desirable conditions are stressed that help make (6) more tractable.
i. Every participating UAV is sufficiently far from both the emitter location and its estimate.
ii. The update interval of UAV state is sufficiently small, resulting in small position change relative to the range with respect to the emitter.
These conditions are intended to uphold the statement that velocity updates dominantly influence the optimal value in (6). These assumptions are collectively called a *far-field small-interval* condition hereafter.

To show some finer points, discussion from this point on is specialized to a 4-sensor (2-sensor-pair) network. In this case (6) becomes

$$\min_{(x_{ji}, y_{ji}, u_{ji}, v_{ji}), \ i,j=1,2} ln\left|(G_1^T C_1^{-1} G_1 + G_2^T C_2^{-1} G_2)^{-1}\right| \quad (7)$$

where G_i is defined in (3) evaluated at current estimate $(\hat{x}_e, \hat{y}_e)$ with entries

$$G_{11,i} = \frac{1}{c}\left[\frac{x_{2,i} - \hat{x}_e}{\sqrt{(x_{2,i} - \hat{x}_e)^2 + (y_{2,i} - \hat{y}_e)^2}}\right.$$

$$- \frac{x_{1,i} - \hat{x}_e}{\sqrt{(x_{1,i} - \hat{x}_e)^2 + (y_{1,i} - \hat{y}_e)^2}} \Bigg] \quad (8)$$

$$G_{12,i} = \frac{1}{c} \left[\frac{y_{2,i} - \hat{y}_e}{\sqrt{(x_{2,i} - \hat{x}_e)^2 + (y_{2,i} - \hat{y}_e)^2}} - \frac{y_{1,i} - \hat{y}_e}{\sqrt{(x_{1,i} - \hat{x}_e)^2 + (y_{1,i} - \hat{y}_e)^2}} \right] \quad (9)$$

$$\begin{aligned} G_{21,i} = \{ & \frac{(x_{1,i} - \hat{x}_e)\left[(x_{1,i} - \hat{x}_e)u_{1,i} + (y_{1,i} - \hat{y}_e)v_{1,i}\right]}{\sqrt{(x_{1,i} - \hat{x}_e)^2 + (y_{1,i} - \hat{y}_e)^2}^3} \\ & - \frac{(x_{2,i} - \hat{x}_e)\left[(x_{2,i} - \hat{x}_e)u_{2,i} + (y_{2,i} - \hat{y}_e)v_{2,i}\right]}{\sqrt{(x_{2,i} - \hat{x}_e)^2 + (y_{2,i} - \hat{y}_e)^2}^3} \\ & - \frac{u_{1,i}}{\sqrt{(x_{1,i} - \hat{x}_e)^2 + (y_{1,i} - \hat{y}_e)^2}} \\ & + \frac{v_{2,i}}{\sqrt{(x_{2,i} - \hat{x}_e)^2 + (y_{2,i} - \hat{y}_e)^2}} \} \frac{f_e}{c} \end{aligned} \quad (10)$$

$$\begin{aligned} G_{22,i} = \{ & \frac{(y_{1,i} - \hat{y}_e)\left[(x_{1,i} - \hat{x}_e)u_{1,i} + (y_{1,i} - \hat{y}_e)v_{1,i}\right]}{\sqrt{(x_{1,i} - \hat{x}_e)^2 + (y_{1,i} - \hat{y}_e)^2}^3} \\ & - \frac{(y_{2,i} - \hat{y}_e)\left[(x_{2,i} - \hat{x}_e)v_{2,i} + (y_{2,i} - \hat{y}_e)v_{2,i}\right]}{\sqrt{(x_{2,i} - \hat{x}_e)^2 + (y_{2,i} - \hat{y}_e)^2}^3} \\ & - \frac{v_{1,i}}{\sqrt{(x_{1,i} - \hat{x}_e)^2 + (y_{1,i} - \hat{y}_e)^2}} \\ & + \frac{v_{2,i}}{\sqrt{(x_{2,i} - \hat{x}_e)^2 + (y_{2,i} - \hat{y}_e)^2}} \} \frac{f_e}{c} \end{aligned} \quad (11)$$

It is clearly seen that $G_{11,i}$ and $G_{12,i}$ are independent of the sensor velocity variables, whereas $G_{21,i}$ and $G_{22,i}$ are linear in the velocities. Overall, matrix G_i is affine in the velocity variables, and its special structure results in that $|G_1^T C_1^{-1} G_1 + G_2^T C_2^{-1} G_2|$ is quadratic. The far-field small-interval condition is now invoked, which excludes sensor positions from the set of optimization variables in (7). The simplified problem aims to

$$\min_{(u_{ji},v_{ji}) \in \mathcal{R}_{ji},\ i,j=1,2} ln \left|(G_1^T C_1^{-1} G_1 + G_2^T C_2^{-1} G_2)^{-1}\right| \quad (12)$$

Unfortunately, no convexity can be assumed in general despite the significant simplification. However, when UAV$_{ji}$ is considered as a point mass with a maximum speed constraint and a maximum curvature constraint, its reachable set $\mathcal{R}_{ji}$ can be easily calculated by integrating from the initial its velocity up to specified interval T seconds (Shin, 2007). The set of optimal points (u_{11}^*, v_{11}^*), (u_{21}^*, v_{21}^*), (u_{12}^*, v_{12}^*), and (u_{22}^*, v_{22}^*) that solves (12) is searched in $\mathcal{R}_{11} \times \mathcal{R}_{21} \times \mathcal{R}_{12} \times \mathcal{R}_{22}$.

3.2 Tolerance to sensor loss

One important contribution of this paper is to support the proposed measures to increase network tolerance to loss of sensors in (Wu, et al., 2008) through numerical simulations, where such tolerance is enhanced in two ways. They are the use of a weighted sum of objective functions by the probability of sensor loss of the form in (6), and the practice to pair the remaining sensors who have lost partners.

Let $\{p_i\}$ be the probability distribution for the surviving network at the end of an update period. A distinct expression of guidance criterion J_i can be be written for each viable outcome of a particular set of surviving sensors based on the information of a single sensor loss probability (Wu, et al., 2008). The modified criterion

$$\begin{cases} \arg \min_{x_{ji}, y_{ji}, u_{ji}, v_{ji}} \ p_1 J_1 + p_2 J_2 + ... + p_k J_k \\ \text{Subject to}: (x_{ji}, y_{ji}, u_{ji}, v_{ji}) \in \mathcal{R}_i,\ j = 1, 2,\ i = 1, \cdots, k \end{cases} \quad (13)$$

is expected to be tolerant to loss of sensors. The details and the benefits of such measures of tolerance to sensor loss are best understood through explanation of results of simulations in the following section. The difficulty caused by the additional cross terms in the measurement error covariance due to reconfiguration in the second case is overcome by using a block diagonal upper bound of the covariance (Wu and Fowler, 2006) in sensor state updates as discussed in Wu et al. [2008].

4. SIMULATION RESULTS

4.1 Location accuracy enhancement through sensor state optimization

The first objective of the simulation study is to verify that the entropy criterion can improve the estimation accuracy. Again a 4-sensor network is used. The signal to noise ratio of the received data is between 15 dB and 20 dB. The true position of the emitter is at the origin and the initial estimate of the emitter location is randomly selected within a 50 × 50 meter rectangle centered at the origin The initial sensor positions are 500 ∼ 1000 meters away from the initial estimate of the emitter location, and the initial UAV velocities are randomly assigned, with a speed between 120 and 140 m/s, and a random direction. Maximal velocity and acceleration are predefined as $140m/s$ and $10m/s^2$ respectively. The Gauss-Newton method (Denis, 1977) is used to calculate the location estimate. Vehicle state update interval is 2 seconds.

To compare the accuracy of the location estimation, 50% error ellipses are formed with and without the sensor state adjustments with 150 independent replications in each case. The best states are selected using the entropy-based criterion defined in (6). Adjusted states are obtained by generating a large number of candidate random states in the reachable set and selecting one state with the lowest entropy value.

Fig. 1 compares the estimation accuracy in terms of geometric closeness of the estimated to the true emitter location. Estimates obtained from measurements by the 4 sensors at their initial selected states are shown as red circles and estimates obtained from measurements by the same 4 sensors at their adjusted states are marked by black asterisks using the same initial estimate. These adjusted states are reachable within 2 seconds when constrained to a maximum speed at $140m/s$ and a maximum magnitude of acceleration at $10m/s^2$. Concentration ellipses enclosing 50% of the 150 independent estimates are also shown for each case with matching colors. The improvement in estimation accuracy is evident.

Fig. 2 compares the same two scenarios in terms of their computed entropies for all 150 pairs corresponding to the recent estimates with and without velocity adjustment.

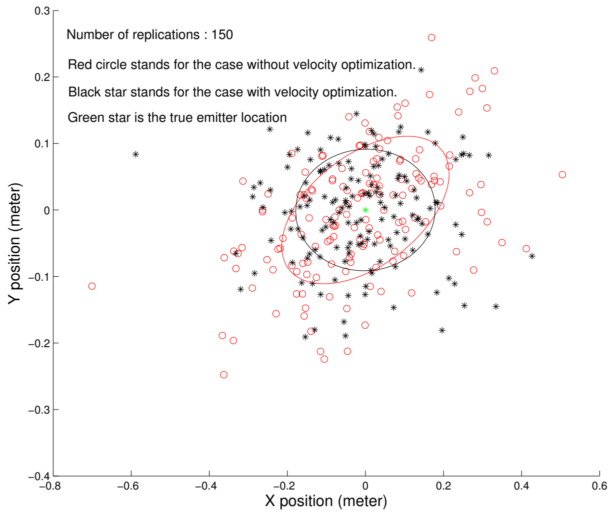

Fig. 1. 150 location estimates without velocity optimization (red circle) and 150 location estimates with velocity optimization (black star)

The results show that, as expected, with the data acquisition at the best reachable states, the distributions of all the 150 estimation error vectors have lower entropies. The more pronounced fluctuation observed in the case where sensor velocities are optimized is due to the logarithmic scale used, and more importantly, the adjusted sensor states can lie outside of the range specified for randomizing the initial sensor states.

4.2 Tolerance to sensor loss through network reorganization

The next set of simulations is aimed at showing the effectiveness of reorganization of the 4-sensor network in the event of loss of one of the sensors. The reorganization simply pairs the remaining sensor that has lost its collaborator with one of the two sensors of the intact pair. The additional complication due to the coupling of the two pairs presented in the estimation error covariance of the

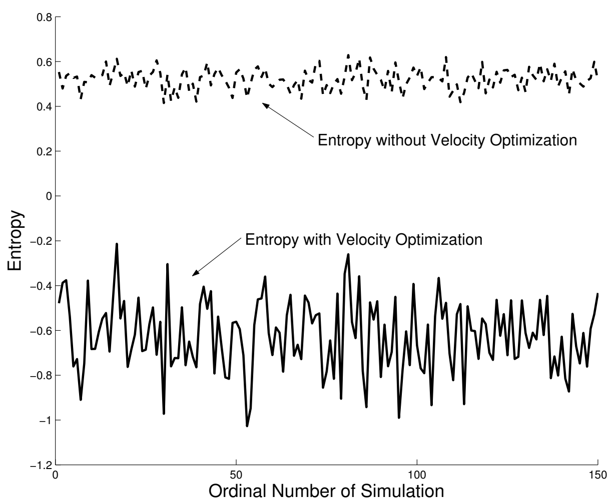

Fig. 2. Accuracy improvement measured by entropy without velocity optimization (dashed line) and entropy with velocity optimization (solid line) in 150 independent replications

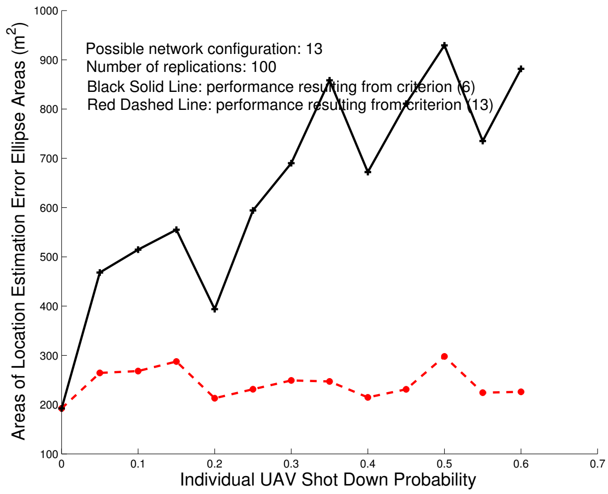

Fig. 3. Comparison of location accuracy resulting from sensor state optimization using probability-weighted criterion equation (13) (red) and unweighted equation (6) (black) as functions of single sensor loss probability

objective function is mitigated by an application of block diagonal upper bound (Wu and Fowler, 2006).

In this simulation, 150 independent replications are performed under the following set of conditions. It is assumed that loss of a sensor is an independent event of a known probability of occurrence within each interval of sensor state update. In particular, a probability of 0.05 is used in the computation and the simulations of this paper. The initial estimate of the emitter location is placed randomly between 2 and 4 kilometers from the emitter. The initial positions the two sensors in each pair are placed randomly 20 to 30 kilometers, and 30 to 40 kilometers from the from the emitter, respectively.

The 4 items shown in Table 1 differ in sensor states and in network configurations. The sample performance column in the table is the sample mean over each of the computed entropies of 150 replications. The numbers in Table 4.2 indicate significant performance recovery through network reorganization upon a sensor loss, despite the conservative estimate of the performance using upper bounding.

4.3 Tolerance to sensor loss through a probability-weighted criterion

This set of simulations is used to compare the location accuracy resulted from optimizing probability-weighted criterion (13) with that resulted from non-weighted criterion (6). 6 sensors (or three pairs) are involved. Signal-to noise ratio is set at $8 \sim 10dB$, maximal speed is set at $150m/s$, maximal acceleration is set at $10m/s^2$, and time

Table 1 : Summary of location accuracy comparison measured by sample means of the calculated entropies of estimated covariances in the distributions of estimation errors of sensor loss-induced configurations of the 4-sensor network.

Network Configuration	Sensor Velocity	Performance
2-pairs, no sensor loss	Initial velocity	3.9703
2-pairs, no sensor loss	optimized under (6)	3.701
2-pairs , 1 sensor loss	optimized under (13)	4.47
1-pair , 1 sensor loss	optimized under (6)	7.459

interval between state update is fixed at 10*seconds*. Initial guess of emitter location is $2.5 \sim 5\ km$ away from the true location. Each UAV is $50 \sim 100\ km$ away from the emitter location. The initial velocity of UAV is $100 \sim 150\ m/s$ with a random direction, and single sensor loss probability within an update interval is varied from $0\% \sim 60\%$.

Figure 3 shows the comparison of the area of 50% concentration ellipses which are equivalent to calculated entropies used in the previous subsection. As expected, the location accuracy with optimal sensor state derived under weighted-criterion (13) is extremely robust with respect to a range of single sensor loss probability, and degrades sharply under (6) as the sensor loss probability increases.

5. CONCLUSIONS AND FUTURE WORK

This paper uses entropy associated with the distribution of the estimate of emitter location as a criterion by which sensor velocities for the next round of TDOA/FDOA data acquisition are optimized. Iteration between emitter location estimation and sensor trajectory update has shown to expedite the target location mission. The entropy criterion was arrived at naturally due to its equivalence to volume minimization of the ellipsoid (or area minimization of ellipse), which is a commonly used measure of location accuracy (Torrieri, 1984).

Tolerance to sensor loss is achieved through two approaches. (i) The entropy criterion used to determine the next sensor velocities is weighed by the probabilities from the distribution of surviving network structures derived from the the single sensor loss probability. (ii) The network is restructured to allow the single remaining sensors to recombine so that they can continue to provide target information after losing their partners.

Time-coordinated control of vehicles to their desired next states is being considered. Algorithms for verification of collision-free condition are also being developed.

REFERENCES

P. C. Chestnut. Emitter Location Accuracy Using TDOA and Differential Doppler, *IEEE Transactions on Aerospace and Electronic Systems*, Vol. AES-18, No. 2, pp. 214-218, March 1982

D. J. Torrieri. Statisal Theory of Passive Location System, *IEEE Transactions on Aerospace and Electronic Systems*, Vol. AES-20, No.2, pp. 183-198, March 1984

R. W. Day and D. R. Oxe. Passive Location Accuracy Via a General Covariance Error Model, *IEEE Aerospace Applications Conference, Feb 12-17 1989, Breckenridge, Colorado, USA*

K. C. Ho and W. Xu. An Accurate Algebraic Solution for Moving Source Location Using TDOA and FDOA Measurements, *IEEE Transactions on Signal Processing*, Vol 52 No.9, pp. 2453-2463, September 2004

I Kaminer, O. Yakimenko, A. Pascoal and R. Ghabcheloo. Path Generation, Path Following and Coordinated Control for Time-Critical Missions of Multiple UAVs, *2006 American Control Conference, June 14-16, 2006, Minneapolis, Minnesota, USA*

O. Yakimenko. Direct method for rapid prototyping of near optimal aircraft trajectories, *AIAA Journal of Guidance, Control, and Dynamics*, pp.865-875, Vol.23. No.5, September-October 2000

S. Stein. Differential Delay Doppler ML Estimation with Unknown Signals, *IEEE Transactions on Signal Processing*, Vol. 41, No. 8, pp.2717-2719, August 1993

S. Kay. *Fundamentals of Statistical Signal Processing, Volume I: Estimation Theory* Chapter 5,11, Prentice Hall, 1993,

M. L. Fowler and M. Chen, Evaluating Fisher Information From Data for Task-Driven Data Compression *40th Annual Conference on Information Sciences and Systems*, Princeton, March 2006

T. M. Cover, J. A. Thomas, and M. T. Burns. *Elements of Information Theory* Wiley & Sons, Inc., Chapter 2,9, c1991 edition

J. Y. Shin. Notes, private communication with N. E. Wu, 2007.

N. E. Wu, Y. Guo, K. Huang, M. C. Ruschmann, and M. L. Fowler Fault-tolerant tasking and guidance of an airborne location sensor network to appear in *Special Issue on Fault Detection, Isolation, and Fault-Tolerant Control, International Journal of Computation, Automation, and Systems*, 2008.

N. E. Wu and M. L. Fowler. An Error bound for sensor fusion with application to Doppler frequency based emitter location *IEEE Transactions on Automatic Control* Page 631-635, 2006

J. E. Dennis Nonlinear Least Squares, State of Art in Numerical Analysis *ed. D. Jacobs, Academic Press*, 1977.